Mon. Not. R. Astron. Soc. **000**, 1–7 (2012) Printed 29 February 2012 (MN LATEX style file v2.2)

Not too big, not too small: the dark halos of the dwarf spheroidals in the Milky Way

Carlos A. Vera-Ciro[1⋆], Amina Helmi[1], Else Starkenburg[1,2] and Maarten A. Breddels[1]

[1] *Kapteyn Astronomical Institute, Univ. of Groningen, P.O. Box 800, 9700 AV Groningen, The Netherlands*
[2] *Dept. of Physics and Astronomy, University of Victoria, PO Box 3055, STN CSC, Victoria BC V8W 3P6, Canada*

29 February 2012

ABSTRACT

We present a new analysis of the Aquarius simulations done in combination with a semi-analytic galaxy formation model. Our goal is to establish whether the subhalos present in ΛCDM simulations of Milky Way-like systems could host the dwarf spheroidal (dSph) satellites of our Galaxy. Our analysis shows that, contrary to what has been assumed in most previous work, the mass profiles of subhalos are generally not well fit by NFW models but that Einasto profiles are preferred. We find that for shape parameters $\alpha = 0.2 - 0.5$ and $v_{\rm max} = 10 - 30$ km/s there is very good correspondance with the observational constraints obtained for the nine brightest dSph of the Milky Way. Furthermore, the internal dynamics of these systems, as well as the number of objects of a given circular velocity are also matched if the total mass of the Milky Way is $\sim 8 \times 10^{11}$ $M_\odot$, a value that is in agreement with many recent determinations. Our simulations show important scatter in the number of bright satellites, even when the Aquarius Milky Way-like hosts are scaled to a common mass, and we find no evidence for a missing population of massive subhalos in the Galaxy. This conclusion is also supported when we examine the dynamics of the satellites of M31.

Key words: cosmology: theory - dark matter.

1 INTRODUCTION

Despite the great success of the ΛCDM concordance cosmological model on large scales, on the scales of galaxies and below the theory is often defied. Some of the issues on small scales have been consistently explained within the theory itself with the inclusion of physical processes that mostly affect baryons. This is the case for the "missing satellite problem" (Klypin et al. 1999), namely the overabundance of satellites in dark matter only simulations compared to the observed number of luminous objects around the Milky Way and other nearby galaxies. It is now widely accepted that the shallow potential wells of small dark matter halos must be strongly affected for example, by reionization, feedback and that star formation is highly inefficient in such systems (Somerville 2002).

Recently, Boylan-Kolchin, Bullock & Kaplinghat (2011a,b) have argued that the dark matter satellites (subhalos herafter) predicted by ΛCDM are persistently too dense to host the observed population of dwarf spheroidal galaxies (dSph) in the Milky Way if these are embedded in halos following Navarro, Frenk & White (1996, 1997, hereafter NFW) profiles. A few studies have been presented in the literature that address this conundrum. Lovell et al. (2011) showed that in warm dark matter cosmological simulations of Milky Way-like halos, the circular velocity curves of subhalos are consistent with those derived by Wolf et al. (2010) for the Milky Way satellites. Following a similar line, Vogelsberger, Zavala & Loeb (2012) carried out simulations of self-interacting dark matter and showed that the most massive subhalos develop cores, what could partially solve the problem. On the other hand, di Cintio et al. (2011) pointed out that by including baryons in the cold dark-matter context the problem becomes more severe probably due to the additional adiabatic contraction experienced by the dark matter subhalos hosting gas.

There are two assumptions implicit in the models which may lead to biased answers if overlooked. These concern (i) the actual mass of the Milky Way and, (ii) the density profiles followed by dark matter satellites assembled in ΛCDM. The first issue has been addressed with a plethora of methods leading to measures that, usually, are consistent with

⋆ E-mail: cavera@astro.rug.nl

a total mass of $0.7 - 2.0 \times 10^{12}$ $M_\odot$ (Wilkinson & Evans 1999; Sakamoto, Chiba & Beers 2003; Battaglia et al. 2005, 2006; Smith et al. 2007; Li & White 2008; Xue et al. 2008; Kallivayalil et al. 2009; Guo et al. 2010; Watkins, Evans & An 2010). The measurements suffer from uncertainties in the modelling as well as limitations in the kinematics of the tracers used. Therefore comparisons to simulations of Milky Way dark matter halos should take into account this uncertainty.

On the second issue, namely the density profile of subhalos, significant progress has been made, especially in recent years. Already Stoehr et al. (2002) found that the circular velocity curves of subhalos in cosmological N-body simulations are more narrowly peaked (in a log-log plot) than the widely used NFW models. The outstanding numerical resolution achieved in the latest of such cosmological N-body simulations has enabled a closer examination of the shape of the density profile down to the innermost few parsecs of dark matter halos (Springel et al. 2008; Madau, Diemand & Kuhlen 2008). Such studies have shown that Einasto models provide better matches to the density profiles found in the simulations than the NFW form(Navarro et al. 2010; Reed, Koushiappas & Gao 2011).

In this paper, we will reconsider both these issues and establish how much they affect the conclusions drawn by Boylan-Kolchin, Bullock & Kaplinghat (2011b). Like these authors we use the Aquarius halos, but we supplement the dynamical information provided by the simulations with a semi-analytic galaxy formation model (Starkenburg et al. in prep). One of the advantages of this approach is that it enables us to directly compare objects in the simulation with those observed. We introduce some relevant features of the simulations in Section 2, while in Section 3 we present in detail the results of our analysis. We draw our conclusions in Section 4.

2 NUMERICAL PRELIMINARIES

We use the simulations of the Aquarius project, six Milky Way-sized dark matter halos assembled in a background cosmology consistent with the constraints yielded by WMAP-1. Each halo (labeled from `A` to `F`) was simulated at different resolutions, starting from a particle mass $m_p = 3.143 \times 10^6$ $M_\odot$ for the lowest and $m_p = 1.712 \times 10^3$ $M_\odot$ for the highest resolution. In what follows we focus on the level `2` which is the highest level at which *all* the Aquarius halos were simulated (For more details see Springel et al. 2008).

Subhalos in these simulations are identified as bound overdensities with SUBFIND (Springel et al. 2001). For each subhalo we compute the circular velocity profile as $v_c^2(r) = Gm(r)/r$, where $m(r)$ is the mass enclosed within the spherical radius r. The maximum circular velocity $v_{\rm max}$ is defined as the peak of the circular velocity curve, and is reached at position $r_{\rm max}$, i.e. $v_c(r_{\rm max}) = v_{\rm max}$.

Numerical convergence is established by looking at the convergence radius as defined by Power et al. (2003). Navarro et al. (2010) showed that the roots of the equation

$$\kappa = \frac{\sqrt{200}}{8} \frac{n(r)}{\ln n(r)} \left[\frac{\overline{\rho}(r)}{\rho_c} \right]^{-1/2}, \qquad (1)$$

correspond to different degrees of convergence depending on the value of the parameter κ. In this equation $n(r)$ is the number of particles enclosed within the radius r and $\overline{\rho}(r)/\rho_c$ is the spherical density at this position in units of the critical value. Comparing the various resolutions of the Aquarius simulations, Navarro et al. (2010) showed that $\kappa = (7.0, 1.0, 0.4)$ correspond to deviations in the circular velocity profile of about $(2.5\%, 10\%, 15\%)$ respectively. Here, we use $r_{\rm conv}(\kappa = 0.4)$ for each subhalo. We also define the tidal radius $r_{\rm tidal}$ of a subhalo as that which encompasses 95% of the bound particles. The results from our definition show a good agreement with the output from more sophisticated expressions for the tidal radius (Tormen, Diaferio & Syer 1998).

To make more direct comparisons to the satellite population of the Milky Way, we have also run a semi-analytic model of galaxy formation for all the Aquarius halos. This model is based on that originally developed by Kauffmann et al. (1999); Springel et al. (2001); De Lucia, Kauffmann & White (2004); Croton et al. (2006); De Lucia & Blaizot (2007) and later modified to describe more accurately processes on the scales of dwarf galaxies (Li, De Lucia & Helmi 2010). The implementation used here also includes recipes for stellar stripping and tidal disruption. The resulting satellite luminosity function agrees well with that of the Milky Way as reported by Koposov et al. (2008) (see Section 3.3). Also the internal properties of the satellites, such as scaling relations, metallicities and star formation histories are in good agreement with those observed (for more details see Starkenburg et al. in prep).

3 RESULTS

3.1 About the density profiles

It was recently reported that mass profiles of ΛCDM halos deviate from the NFW functional form. Navarro et al. (2010) showed that a parametric model with a density profile with logarithmic slope described by a power-law (Einasto profile) provides better fits for objects of virial mass $\sim 10^{12}$ $M_\odot$. The power index α adds another free parameter, therefore the fits are expected to improve. Nevertheless, it was shown by Springel et al. (2008) that even after fixing $\alpha = 0.16$ the Einasto profile still yields much better results. The nature of the shape parameter α has been recently investigated for isolated objects with masses in excess of 5×10^{12} $M_\odot$ and the results suggest a deep connection with the pseudo-phase-space density distribution (Ludlow et al. 2011). For smaller objects Springel et al. (2008) also showed that the mass profiles follow much closer the Einasto than the NFW model. For both models, the mass enclosed within the spherical radius r can be written as

$$m(r) = 4\pi r_{-2}^3 \rho_{-2} g(r/r_{-2}), \qquad (2a)$$

where r_{-2} is the radius at which the logarithmic slope of the density profile reaches the isothermal value and ρ_{-2} is the density at that position. The details of each model are inherited by the function g, which takes the form

$$g_{\rm NFW}(x) = 4\ln(1+x) - \frac{4x}{1+x}, \qquad (2b)$$

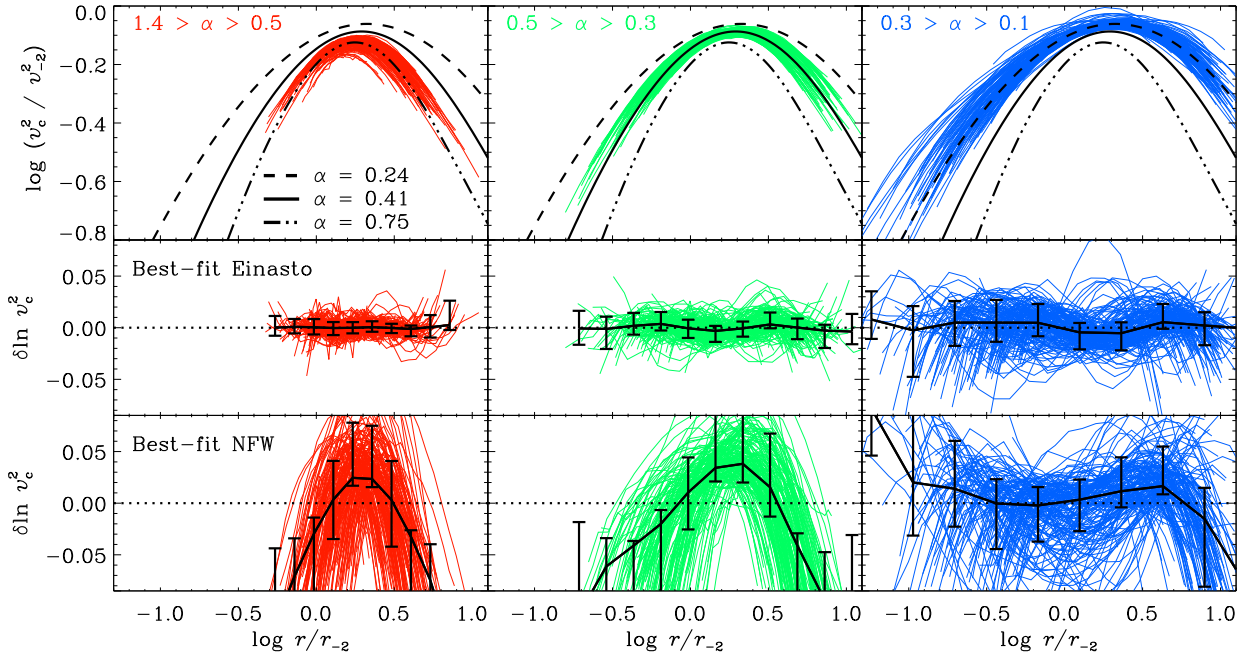

Figure 1. Spherically averaged circular velocity profiles $v_c^2(r) = Gm(r)/r$ for the subhalos that are predicted to host stars by our semi-analytic model. Velocities have been scaled to $v_{-2}^2 \equiv 4\pi G\rho_{-2}r_{-2}^2$. As already reported in Stoehr et al. (2002) the velocity profiles of subhalos tend to be more narrowly peaked than in the NFW form. The sample of subhalos has been grouped according to the best fit value of α, and plotted with different colors. An Einasto profile with the average value of α for each bin is overplotted. The residuals from the best-Einasto (NFW) fits are shown in the middle (bottom) panel, and in general are consistent with zero for the Einasto profile and exhibit systematic deviations from zero for the NFW case. In the column $\langle\alpha\rangle = 0.24$ both models yield similar results, which is naturally expected since the NFW equivalent is reached with $\alpha = 0.22$. The systematic change of $r_{\rm conv}/r_{-2}$ with α is a consequence of setting the convergence parameter κ to a fixed value.

for the NFW profile, and

$$g_{\rm Einasto}(x) = \frac{1}{\alpha}\exp\left(\frac{3\ln\alpha + 2 - \ln 8}{\alpha}\right)\gamma\left(\frac{3}{\alpha}, \frac{2x}{\alpha}\right), \quad (2c)$$

for the Einasto model. Here $\gamma(a, x)$ is the lower incomplete gamma function. Although intrinsically different, these profiles resemble each other for $\alpha \approx 0.22$ in $0.01 \leqslant r/r_{-2} \leqslant 100$. That means that objects that have a shape parameter close to this value are well fitted by either model. Fig. 1 shows the spherically averaged circular velocity profiles $v_c^2 = Gm(r)/r$ for all the subhalos that are predicted to host stars according to our semi-analytical model. In total we calculate 20 bins in the region $r_{\rm conv} \leqslant r \leqslant 0.9\, r_{\rm tidal}$, we use this upper cutoff to ensure that our fits are not driven by tidal effects. All objects have at least 200 particles, but generally significantly more than 1000. For each of the plotted subhalos we calculate the merit function

$$E = \frac{1}{N_{\rm bins}}\sum_{i=1}^{N_{\rm bins}}(\ln v_c^2(r_i) - \ln v_{c,i}^2)^2, \quad (3)$$

and minimize it against the free parameters of each model. We have deliberately chosen to use the cumulative mass instead of the differential profile since it is less sensitive to the shot-noise of each bin, as a consequence we can go to low number of particles, whenever the restriction $n(0.9\, r_{\rm tidal}) - n(r_{\rm conv}) \geqslant 200$ is met.

Fig. 1 shows the results of our fitting procedure. Here the subhalos have been binned according to their best fit α value. The three different columns show the subhalos that fall into each α-bin, the average α within each bin is quoted in the top-left panel. Each curve in the top row has been conveniently normalized to the characteristic velocity $v_{-2}^2 \equiv 4\pi G\rho_{-2}r_{-2}^2$ and the characteristic radius r_{-2}. We have also overplotted the predicted Einasto profiles for the average α. The middle panels show the residuals of the best-Einasto fit for each subhalo, the thick line represent the median and 1σ equivalent dispersion. The residuals are consistent with zero indicating that the Einasto profile fits better than NFW (whose residuals are shown in the bottom panel), especially for large α values. Interestingly, for $\langle\alpha\rangle = 0.24$ the NFW model provides a good and comparable fit to the Einasto model (see bottom-right panel). This is actually expected, since $\alpha = 0.22$ represents a model that nearly follows the NFW profile.

3.2 MW's dSphs constraints revisited

Wolf et al. (2010) have shown that the mass enclosed within the half mass radius $r_{1/2}$ of a dynamical system can be robustly determined as $m_{1/2} = 3G^{-1}\langle\sigma_v^2\rangle r_{1/2}$, without (precise) knowledge of its velocity anisotropy. Here $\langle\sigma_v^2\rangle$ is the light-weighted average line-of-sight velocity dispersion of the system. In the case of dSph galaxies, this effectively implies a measurement of the circular velocity at $r_{1/2}$, which therefore constrains the possible family of circular velocity curves for a given dark matter density profile. Following Boylan-Kolchin, Bullock & Kaplinghat (2011b) we plot in Fig. 2 the 2σ constraints derived in this way for the 9

most luminous dSphs satellites of the MW (i.e. excluding the Sagittarius dwarf galaxy and the Small and Large Magellanic Clouds). Like Boylan-Kolchin, Bullock & Kaplinghat (2011b) here we assume these systems are embedded in NFW profiles, which leads to the gray band shown in the figure. This band is also nearly consistent with the masses enclosed within 300 pc as reported by (Strigari et al. 2008) $2.5 \times 10^6 \leqslant m(300\ \mathrm{pc})/\mathrm{M}_\odot \leqslant 3.0 \times 10^7$.

The advantage of using this plot is that one can directly compare against the results extracted from ΛCDM simulations. The filled circles in Fig. 2 show the distribution of $(r_{\rm max}, v_{\rm max})$ measured directly from our simulations for the satellites hosting stars. The colors indicate the predicted luminosities and the sizes correspond to the bound mass fraction at present day, i.e. $f_{\rm bound} = m(0)/m(z_{\rm infall})$, where $z_{\rm infall}$ is the lowest redshift at which the progenitor of a given subhalo was not associated to one of the main Aquarius halos. Here, the values $(r_{\rm max}, v_{\rm max})$ have been corrected for softening length effects following the expressions given by Zavala, Springel & Boylan-Kolchin (2010). As highlighted in the Introduction, there are important differences in the location of the points from the simulations and those derived for the dSph satellites of the Milky Way, which may lead to the conclusion that there is a significant problem with our currently preferred cosmological model.

However, this comparison may be need to be revisited since we demonstrated in the previous section that an NFW profile is not expected to describe well the dark matter halos of satellites in ΛCDM. Therefore, we have computed the family of $(r_{\rm max}, v_{\rm max})$ values that are consistent with the measurement of $v_c(r_{1/2})$ for the dSph of the Milky Way, but now we have considered Einasto profiles. The 2σ constraints are shown in Fig. 2. Given the freedom we have in choosing the extra parameter α (this is still unconstrained by the observations), we have plotted 3 different bands corresponding to $\alpha = (0.22, 0.30, 0.50)$. The $\alpha = 0.22$ (solid lines) is consistent with the NFW predictions, as expected. For larger values of α the constraints from observations actually overlap with those found in the simulations. For $\alpha = 0.5$ (dashed line) the match is almost perfect.

Fig. 2 shows that there is a correlation between the value of α and $f_{\rm bound}$ i.e. the amount of stripping a subhalo has experienced. Very heavily stripped objects have, on average, higher α, and deviate the most from NFW profiles. The black dots in this figure correspond to the location of isolated dark matter halos in the same $v_{\rm max}$ range as the satellites. This confirms that such isolated dark matter halos are well-fit by NFW profiles, and that tidal stripping is acting on the subhalos to change the shape of their circular velocity profile to the Einasto form (see also Hayashi et al. 2003).

The Milky Way does not have many very luminous dwarf galaxy satellites. Brighter than Fornax ($M_V \sim -13.2$), only the Sagittarius dwarf and the Magellanic Clouds are known, and none is included in Fig. 2. According to our semi-analytic model such luminous objects would populate the upper-right of this plot, i.e. $v_{\rm max} \gtrsim 40$ km/s and $r_{\rm max} \gtrsim 2.5$ kpc. Therefore, although the mismatch between the observations (with the assumption of NFW, Boylan-Kolchin, Bullock & Kaplinghat 2011a) and the simulations might be alleviated using an Einasto profile, in this region of the diagram, the difference may be entirely attributed to the absence of other bright dSph in the Milky Way. It is the region with $v_{\rm max} \sim 20 - 40$ km/s, where we expect to find the subhalos hosting most of the classical dSph according to this plot, where the difference between assuming an NFW or an Einasto profile needs to be taken into account to bring the simulations in agreement with the observations.

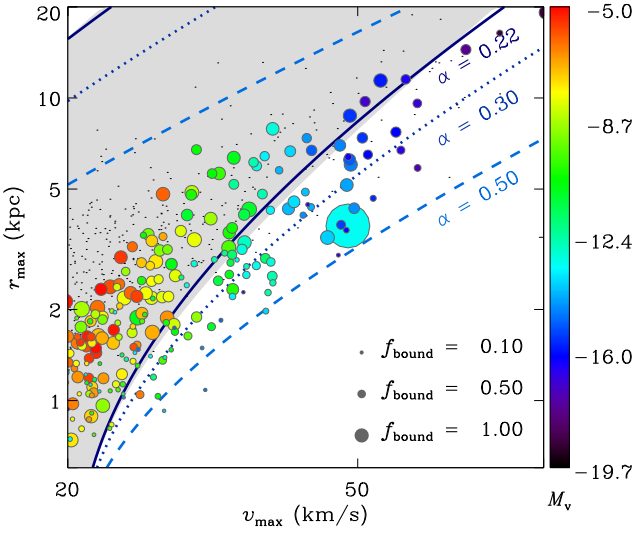

Figure 2. Constraints for the MW's dwarf spheroidals using NFW (gray band) and Einasto (blue curves) profiles. Points are the results from the six Aquarius halos, colored according to their predicted luminosity and sized using the fraction of mass retained after infall. The black dots correspond to isolated halos in the simulations.

3.3 Effects of the host halo mass

Springel et al. (2008) have shown that the mass function of dark matter halos is independent of mass, i.e. that it is self-similar. This implies that the number of subhalos of a given mass scales directly with the mass of the host (although Gao et al. 2012, suggest that the slope is slightly larger for 10^{15} $\mathrm{M}_\odot$ objects). Therefore, we can expect that, down to a certain scale, brighter or more massive central galaxies will host a larger number of satellites. This is indeed shown in the top panel Fig. 3, where we have plotted the luminosity function of all Aquarius halos. It is clear from this figure that this is the case, since the three heavier of the Aquarius halos `Aq-A-2`, `Aq-C-2` and `Aq-D-2` have 57, 62 and 67 satellites respectively, while the lightest, `Aq-B-2` has only 36 satellites with $M_v \leqslant -5$, and hence has the shallowest luminosity function in the faint end. It is possible to show that a doubling of the mass of the host halo roughly leads to an increase by a factor of ~ 2 in the number of satellites brighter than $M_v = -5$ (Starkenburg et al. in prep).

We thus explore the effect of host halo mass on the properties of our simulated satellites, by re-scaling all halos to a common value following Helmi, White & Springel (2003). Because of the scale-free nature of gravity, we may assume that if a halo of mass $M_{\rm Aq}$ is scaled to have a mass

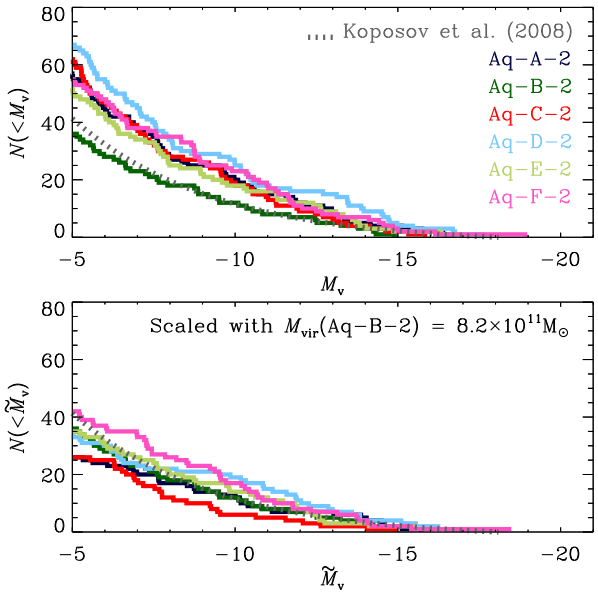

Figure 3. Luminosity function for the original Aquarius simulations (top) and once they have scaled to the mass of `Aq-B-2` (bottom). For reference we have added the observed luminosity function for the Milky Way as derived by Koposov et al. (2008). Although in the scaled version the simulations follow much more closely the observations, some differences remain in the number of satellites of a given luminosity.

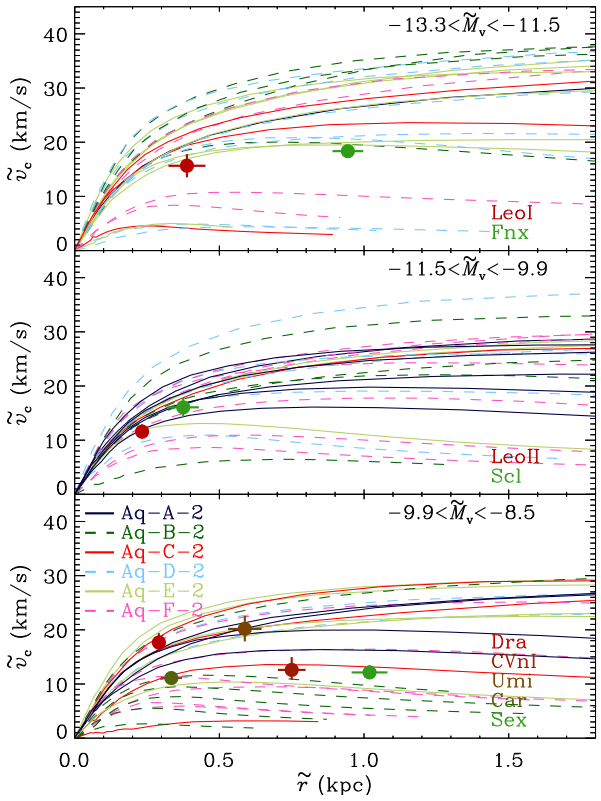

Figure 4. Circular velocity profiles for scaled subhalos in three different luminosity bins, following the absolute magnitudes of the nine classical dSph of the Milky Way. The subhalos are colored according to the host halo they are associated with. This figure shows that the number of satellites per bin, as well as the velocities profiles are consistent with the measurements obtained for the dSph.

$M_{\rm MW}$ then the subhalos's masses m should be scaled as

$$\widetilde{m} = m\frac{M_{\rm MW}}{M_{\rm Aq}} \equiv \mu m. \tag{4a}$$

Naturally the distances will become

$$\widetilde{r} = \mu^{1/3} r, \tag{4b}$$

while the circular velocity profiles

$$\widetilde{v_c} = \left(\frac{G\widetilde{m}}{\widetilde{r}}\right)^{1/2} = \mu^{1/3} v_c. \tag{4c}$$

To determine the factor $\mu \equiv M_{\rm MW}/M_{\rm Aq}$, we need to specify $M_{\rm MW}$. As discussed in the Introduction, the value of the total mass of the Milky Way is quite uncertain. However, motivated by the remarkable match between the luminosity function of `Aq-B-2` and that of the Milky Way (Koposov et al. 2008), we set $M_{\rm MW} = M_{\rm vir}(\texttt{Aq-B-2}) = 8.2\times10^{11} M_\odot$[1]. This value is consistent with many recent studies using different techniques (e.g. Battaglia et al. 2005, 2006; Smith et al. 2007; Xue et al. 2008). This implies that the value of μ ranges from unity to 2.2 at most, which implies that distances and velocities in the scaled simulations will be at most decreased by a factor of 1.3.

We run our semi-analytic galaxy formation model now for the re-scaled Aquarius simulations. The resulting luminosity function is shown in the bottom panel of Fig. 3, where the new predicted magnitudes are denoted by $\widetilde{M}_v$. It is evident from this figure that each halo now follows much more closely the Milky Way's luminosity function. It is important to note that there is still some halo-to-halo dispersion, which can be attributed to the stochastic nature of the mass assembly of each object. That is, not all the galaxies with the same mass are expected to have the same number of satellites with the same luminosity, although some form of statistical equivalence should be present.

We now study more closely the circular velocity profiles of the subhalos hosting satellites, since previous works have highlighted a discrepancy between the observations and the simulations (Boylan-Kolchin, Bullock & Kaplinghat 2011b; Lovell et al. 2011). Fig. 4 shows the scaled circular velocity profiles for all the subhalos hosting satellites with luminosities in the quoted range. As in previous sections, we have also included the estimates for the 9 most luminous dSphs of the Milky Way following Wolf et al. (2010). The first conclusion is that our semi-analytic model places (satellite) galaxies of a given luminosity in the right mass (sub)halos, since the amplitude of the rotation curves in all cases are consistent with those observed. Secondly, the number of objects per luminosity bin is in good agreement with the number observed, as established in Fig. 3. For example, in the most luminous bin (top panel) the median number of bright satellites per halo is 3, while for intermediate luminosities it is 4, and for the faintest considered here, it is 4. We em-

[1] In this paper we denote $M_{\rm vir} = M_{200}$, i.e. the the mass enclosed in a sphere with mean density 200 times the critical value.

dSph	$N\sigma$ away	Observed $v_c(r_{1/2})$	Median $v_c(r_{1/2})$	med(v_c) -1σ	med(v_c) $+1\sigma$
Fnx	-0.72	18.3	25.4	6.0	32.0
LeoI	-0.73	15.7	19.4	8.2	24.5
Scl	-0.47	16.1	17.6	12.8	20.8
LeoII	-1.03	11.6	14.2	11.9	16.8
Sex	-0.22	12.1	16.4	4.4	25.3
Car	-0.40	11.1	13.6	6.6	20.0
Umi	$+0.62$	20.2	16.2	5.8	22.4
CVnI	-0.23	12.6	16.3	5.1	23.0
Dra	$+1.03$	17.7	13.6	6.7	17.6

Table 1. Statistical comparison of the 9 most luminous classical dSphs with the simulated velocity profiles in Fig. 4.

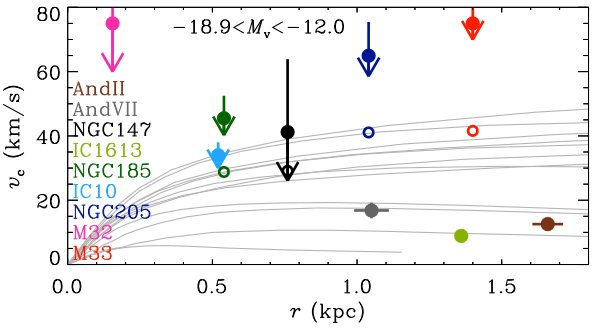

Figure 5. Circular velocities for the subhalos present in halo `Aq-C-2` associated to satellites with luminosities $M_v \leqslant -12$. The symbols represent observations of the satellites of M31 in the same luminosity range. Open symbols represent the estimated dark matter contribution to $v_c(r)$ when the decomposition is available (see text for details).

phasize however that the range within a given luminosity bin is quite broad. For example for the brightest bin, the scaled `Aq-A-2` has just 1 satellite, while the scaled `Aq-D-2` has 7. Such large variations are not unexpected, but stresses that strong conclusions cannot be drawn when the number of objects is so small as in the case of the bright end of the luminosity function.

The galaxies shown in the fainter two bins agree quite well with the predictions of our models. There is no systematic mismatch, with the dSph circular velocity measurements at the half-light radius lying close to the median velocity profile of the simulated satellites. An apparent discrepancy is present in the most luminous bin $-13.2 \leqslant \widetilde{M}_v \leqslant -11.9$ in the sense that there is a larger number of subhalos with circular velocities above the measured values for Fnx and Leo I than there is below. Nevertheless as discussed above, this comparison is limited by statistics and affected by stochastic aspects in the luminosity function.

We quantify this by comparing the observed value of the circular velocity at $r_{1/2}$ for each dSph, with the probability distribution function of v_c calculated at the same radius using all the subhalos that lie in the corresponding luminosity bin. We compute the median v_c and two percentiles of the distribution, namely a lower (15.9%) and an upper (84.1%) value, which would correspond to $\pm 1\sigma$ in the case of a Gaussian. The results of this experiment are shown in Table 1 for the different satellites. Note that here we have translated the probability into an "equivalent" $N\sigma$ away from the median. The table shows that all satellites are consistent with being drawn from the population of subhalos hosting galaxies found in our simulations.

Thus far we have focused on the nine classical dSph, and have excluded from the analysis the Sagittarius dwarf and the Magellanic Clouds. One of the questions originally posed by Boylan-Kolchin, Bullock & Kaplinghat (2011a) is that there may be a hidden population of very massive subhalos in the Milky Way, since the circular velocities of the classical dwarfs are lower than those found for the nine most massive (at infall) subhalos in any of the Aquarius simulations. So far we have shown that our model predicts the satellites of a given luminosity to be hosted in subhalos of the right mass, when comparing to the classical dSph. However we also need to explore what happens for systems brighter than Fnx, and whether we indeed expect a missing population from our models. As expected, the scaled Aquarius halos show a diverse number of systems with $\widetilde{M}_v < -14$, ranging from 2 for `Aq-C-2` to 5 for `Aq-A-2`. A simple comparison to the Milky Way satellite system would suggest that we cannot argue that there is a population of massive satellites that is missing.

As suggested by multiple authors, the dark matter mass of M31 is almost as twice that of the Milky Way (e.g. Li & White 2008; Kallivayalil et al. 2009; Guo et al. 2010; Watkins, Evans & An 2010). This would imply that M31 should host more, and also brighter, satellites than the Milky Way itself. This indeed appears to be the case, as M31 has 9 satellites brighter than Leo I ($M_v = -11.9$) compared to 2 (or 5 when Sgr and the Magallenic Clouds are included) for the Milky Way.

Aquarius halo `Aq-C-2` has $M_{\rm vir} = 1.77 \times 10^{12}$ M$_\odot$ which is ~ 2.2 times larger than our candidate for the Milky Way, making this object a good match for M31. In Figure 5 we show the velocity profiles of all the nine satellites in `Aq-C-2` with $M_v \leqslant -12$. We have also included measurements for M31's satellites with luminosities in that range. It is important to bear in mind that these measurements have been derived using a variety of methods that range from HI rotation curves for IC10 (Wilcots & Miller 1998) and M33 (Corbelli 2003), to 3 integral dynamical modelling for NGC147, NGC185 and NGC2005 De Rijcke et al. (2006). For the dSph AndII and AndVII the method presented by Wolf et al. is used to estimate $v_c(r_{1/2})$ (Kalirai et al. 2010), while for M32 the mass is derived through Jeans modelling (Magorrian & Ballantyne 2001). Many of these bright dwarf galaxies are not as dark matter dominated within the region populated by the stars as the dSph, and hence a direct comparison to the circular velocity of the subhalos is not quite correct. For example, for NGC147, NGC185 and NGC2005 the dark matter content is estimated to be 50%, 40% and 40%, respectively (De Rijcke et al. 2006). The open symbols in Fig. 5 correspond thus to the dark matter contribution to the circular velocity as estimated by these authors, while the solid points represent the total enclosed mass at the given radius. Clearly for M32, a very compact dwarf elliptical, the shown circular velocity is also an upper limit for the dark matter contribution.

This comparison shows that the velocity profiles for our most luminous satellites in `Aq-C-2` are very consistent with

the observations of the dwarfs in M31 over a similar luminosity range. We therefore must conclude there is no evidence of a missing population of very massive of dark satellites.

4 CONCLUSIONS

We have used the state of the art cosmological N-body simulations of Milky Way-like dark matter halos of the Aquarius project, supplemented with a semi-analytic galaxy formation model, to study the dynamical properties of the satellite population in the Local Group.

We have found that the mass profiles of the subhalos associated to bright satellites according to our model deviate from the standard NFW form (see also Stoehr et al. 2002), and that Einasto profiles provide much better fits. The shape parameter α exhibits a correlation with the amount of mass stripped since the time of accretion, indicating that tidal effects may be responsible for the changes in the profiles of dark matter halos once they become satellites (Hayashi et al. 2003).

The comparison of our models to current measurements of the mass enclosed within the half mass radius for the classical dwarf spheroidals suggests that they are embedded in dark matter halos of $v_{\rm max} \sim 10-30$ km/s with $\alpha \sim 0.2-0.5$. In principle, this prediction for the values of the shape parameter α could be tested observationally. However this requires very extensive sampling of the kinematics of stars near the center of the dwarf galaxies. It is also necessary to perform more sophisticated dynamical models, that are free of assumptions regarding the velocity anisotropy of the systems. For example Schwarzschild models of the Sculptor dSph constrain the inner logarithmic slope of the dark matter density profile to be $d\log\rho/d\log r > -1.5$ (Breddels et al. 2012). Better constraints could be obtained if the sample size were increased by a factor ~ 10.

We have also shown that the number and internal dynamics of the classical dSph in the Milky Way are consistent with the predictions of the ΛCDM model, if the Milky Way's mass is $\sim 8 \times 10^{11}$ M$_\odot$. This value well within the range measured using the dynamics of stellar tracers, but suffers from significant uncertainties. However, it is important to note that this low value lowers the probability of a galaxy like the Milky Way to host two satellites as bright as the Small and Large Magellanic Clouds (Busha et al. 2011; Boylan-Kolchin et al. 2010), although such systems appear to be rare in any case, as shown by Liu et al. (2011) using the Sloan Digital Sky Survey.

We have also found significant scatter in the number of subhalos expected to host bright satellites for the Aquarius halos, even when scaled to a common mass of 8×10^{11} M$_\odot$. For example, the scaled `Aq-A-2` has five satellites brighter than Fornax, while the scaled `Aq-C-2` has only two (making it consistent with our Galaxy). Therefore, care should be taken to draw strong conclusions from this region of the luminosity function since the number of objects is small and heavily influenced by the host mass as well as by stochastic effects associated to particular histories. Another example that emphasizes this point is given by M31, which is nearly a factor of two more massive than the MW, and also has a larger number of bright satellites. Just like for the Milky Way, our models for the satellite population of M31 are consistent with the observational constraints on the internal dynamics of the brighter satellites, after taking into account the differences in host mass. Hence we must conclude that we have found no evidence of a missing massive satellite problem in the Local Group.

ACKNOWLEDGMENTS

The Aquarius simulations have been run by the VIRGO consortium, and we are very thankful to this collaboration, and especially indebted to Volker Springel. We are very grateful to Gabriella De Lucia and Yang-Shyang Li in relation to the semi-analytic model of galaxy formation, and to Simon White for a critical reading of the manuscript. AH gratefully acknowledges financial support from the European Research Council under ERC-Starting Grant GALACTICA-240271. ES is supported by the Canadian Institute for Advanced Research (CIfAR) Junior Academy and a Canadian Institute for Theoretical Astrophysics (CITA) National Fellowship.

This paper has been typeset from a TEX/ LATEX file prepared by the author.

REFERENCES

Battaglia G. et al., 2005, MNRAS, 364, 433
Battaglia G. et al., 2006, MNRAS, 370, 1055
Boylan-Kolchin M., Bullock J. S., Kaplinghat M., 2011a, arXiv:1111.2048
Boylan-Kolchin M., Bullock J. S., Kaplinghat M., 2011b, MNRAS, 415, L40
Boylan-Kolchin M. et al., 2010, MNRAS, 406, 896
Breddels M. A. et al., 2012, Assembling the Puzzle of the Milky Way, Le Grand-Bornand, France, Edited by C. Reylé; A. Robin; M. Schultheis; EPJ Web of Conferences, Volume 19, id.03009, 19, 3009
Busha M. T. et al., 2011, ApJ, 743, 117
Corbelli E., 2003, MNRAS, 342, 199
Croton D. J. et al., 2006, MNRAS, 365, 11
De Lucia G., Blaizot J., 2007, MNRAS, 375, 2
De Lucia G., Kauffmann G., White S. D. M., 2004, MNRAS, 349, 1101
De Rijcke S. et al., 2006, MNRAS, 369, 1321
di Cintio A. et al., 2011, MNRAS, 417, L74
Gao L. et al., 2012, arXiv:1201.1940
Guo Q. et al., 2010, MNRAS, 404, 1111
Hayashi E. et al., 2003, ApJ, 584, 541
Helmi A., White S. D. M., Springel V., 2003, MNRAS, 339, 834
Kalirai J. S. et al., 2010, ApJ, 711, 671
Kallivayalil N. et al., 2009, ApJ, 700, 924
Kauffmann G. et al., 1999, MNRAS, 303, 188
Klypin A. et al., 1999, ApJ, 522, 82
Koposov S. et al., 2008, ApJ, 686, 279
Li Y.-S., De Lucia G., Helmi A., 2010, MNRAS, 401, 2036
Li Y.-S., White S. D. M., 2008, MNRAS, 384, 1459
Liu L. et al., 2011, ApJ, 733, 62
Lovell M. R. et al., 2011, MNRAS, 341
Ludlow A. D. et al., 2011, MNRAS, 415, 3895
Madau P., Diemand J., Kuhlen M., 2008, ApJ, 679, 1260

Magorrian J., Ballantyne D., 2001, MNRAS, 322, 702
Navarro J. F., Frenk C. S., White S. D. M., 1996, ApJ, 462, 563
Navarro J. F., Frenk C. S., White S. D. M., 1997, ApJ, 490, 493
Navarro J. F. et al., 2010, MNRAS, 402, 21
Power C. et al., 2003, MNRAS, 338, 14
Reed D. S., Koushiappas S. M., Gao L., 2011, MNRAS, 415, 3177
Sakamoto T., Chiba M., Beers T. C., 2003, A&A, 397, 899
Smith M. C. et al., 2007, MNRAS, 379, 755
Somerville R. S., 2002, ApJL, 572, L23
Springel V. et al., 2008, MNRAS, 391, 1685
Springel V. et al., 2001, MNRAS, 328, 726
Starkenburg E. et al., in prep,
Stoehr F. et al., 2002, MNRAS, 335, L84
Strigari L. E. et al., 2008, Nature, 454, 1096
Tormen G., Diaferio A., Syer D., 1998, MNRAS, 299, 728
Vogelsberger M., Zavala J., Loeb A., 2012, arXiv:1201.5892
Watkins L. L., Evans N. W., An J. H., 2010, MNRAS, 406, 264
Wilcots E. M., Miller B. W., 1998, AJ, 116, 2363
Wilkinson M. I., Evans N. W., 1999, MNRAS, 310, 645
Wolf J. et al., 2010, MNRAS, 406, 1220
Xue X. X. et al., 2008, ApJ, 684, 1143
Zavala J., Springel V., Boylan-Kolchin M., 2010, MNRAS, 405, 593